Imaging of the Paranasal Sinuses and In-Office CT

Paul D. Campbell, Jr, MD, S. James Zinreich, MD*, Nafi Aygun, MD

KEYWORDS

- Imaging for FESS • Sinus anatomy • Sinusitis
- Cone beam CT • CT dose-Index

Since the introduction of functional endoscopic sinus surgery (FESS) in the United States in 1985, the information gained from imaging of the nasal cavity and paranasal sinuses has proved imperative in understanding the regional morphology and guidance of surgical procedures. This regional morphology can vary significantly from patient to patient, and one quickly becomes aware of the fact that ''no two noses are alike.''

Given the need for accurate and detailed display of the nasal cavity and paranasal sinus anatomy, the commonly used imaging technology in 1985, standard plain films and polytomography, was quickly replaced with CT. Coronal CT scans afforded improved resolution of the bony framework and the superimposed mucosa in addition to regional inflammatory pathology. The application of multiplanar reconstruction and then 3-D imaging subsequently provided a more 3-D understanding of the CT imaging data.

In 1991 a significant advance in the use of imaging information to help guide surgeons in the performance of FESS was accomplished with the introduction of image-guided surgery. The imaging data were used to register a patient's location on the operating table with the patient's imaging data in a computer, which then was able to show the location of the surgeon's instruments in the operating field. Surgical accuracy and safety were significantly advanced.

More than 20 years after the introduction of FESS in the United States, the importance of imaging for surgeons continues to be the anatomic detail afforded by this technology, the roadmap it provides in planning the surgery, and the morphologic detail it provides in patients with recurrent disease after surgery. When considering the need to distinguish between various pathologic entities, MRI information can be added to CT information, because its soft tissue resolution is superior to CT.

The Russell H. Morgan Department of Radiology and Radiological Sciences, The Johns Hopkins Medical Institutions, 600 North Wolfe Street/Phipps B-112, Baltimore, MD 21287, USA
* Corresponding author.
E-mail address: sjzinreich@jhmi.edu (S.J. Zinreich).

Otolaryngol Clin N Am 42 (2009) 753–764
doi:10.1016/j.otc.2009.08.015 **oto.theclinics.com**
0030-6665/09/$ – see front matter

The latest development in CT technology is cone beam CT (CBCT) instrumentation.[1] This is a miniaturized CT scanner providing sufficient resolution to outline the maxillofacial bony architecture, and therefore the nasal cavity and paranasal sinus morphology. This scanner requires little space, is easy to operate, emits reduced radiation, and can easily fit in an office setting. This equipment may change the way imaging of the nasal cavity and paranasal sinuses will be performed in the future. These developments are the topics discussed in this article.

CT TECHNIQUE

Single-channel CT scanners use incremental or helical acquisition schemes for paranasal sinus examinations. Image acquisition in the coronal plane is preferred for optimal display of the anterior osteomeatal unit. The slice thickness should be 3 mm or less without interslice gap for optimal evaluation. Image acquisition in the coronal plane may require extension of the head, which may not be possible for some elderly patients and patients with airway problems or neck pain. Thin axial images can be reconstructed in the coronal plane for such patients.

Multidetector CT (MDCT) scanners (also called multichannel or multislice CT scanners) use multiple rows of detectors that allow registration of multiple channels of data with one rotation of the x-ray tube. For example, a 16-slice MDCT scanner has a 16-fold capacity for collecting image data per x-ray tube rotation compared with a single-channel CT. Currently, 64-channel CT scanners are in routine clinical use. A head-to-toe CT scan with slices as thin as 0.2 mm can be obtained in 60 seconds. Recently, 312-channel scanners have been introduced that can image the same volume of tissue over and over again in a short time affording the physiologic studies of heart motion, myocardial perfusion, and brain perfusion. Thin slices permit isotropic data sets, in which the voxels (the smallest elements of a data set) are cubical. Isotropic voxels afford excellent reconstruction of images in essentially any desired plane without degradation of image quality. Isotropic imaging created a paradigm shift in CT imaging, no longer limited by the plane of acquisition. Data can be collected from a body part in any desired plane and 2-D images in any desired plane (multiplanar reconstruction) can be reconstructed (**Fig. 1**). Real-time interactive manipulation of image data and 3-D reconstructions are made possible by high-performance workstations equipped with special software.

In the MDCT scanners, the x-ray beam is collimated to the thickness of the detector row making it a fan-shaped beam.

Flat panel–based/CBCT scanners were recently introduced for routine clinical use. Instead of rows of detectors, these use detectors arranged in a flat surface to capture the x-ray, which is not collimated to a fan shape but rather takes the form of a cone. These scanners have changed the image acquisition paradigm once again. Flat panel–based CT, instead of building the volume from individual slices, acquires the image data volume directly. This provides seamless volume images, which improve 2-D and 3-D reconstructions and model-building capability for presurgical evaluation.

The x-ray source and the detector rotate around a fixed region of interest. The flat panel area detector permits a wider Z-axis coverage compared with a CT slice, allowing coverage of large areas in just one turn of the gantry, with enough data acquired to permit image reconstruction. A CBCT system (**Fig. 2**) has some advantages over traditional MDCT, including decreased cost and radiation exposure. It also has inherent disadvantages, however, which include poor soft tissue contrast resolution due to noise from scatter radiation. Modern MDCT scanners have a contrast resolution of 1 Hounsfield unit (HU), which is 10 times better than that afforded by CBCT scanners. This remains the most significant barrier in widespread clinical use of CBCT.

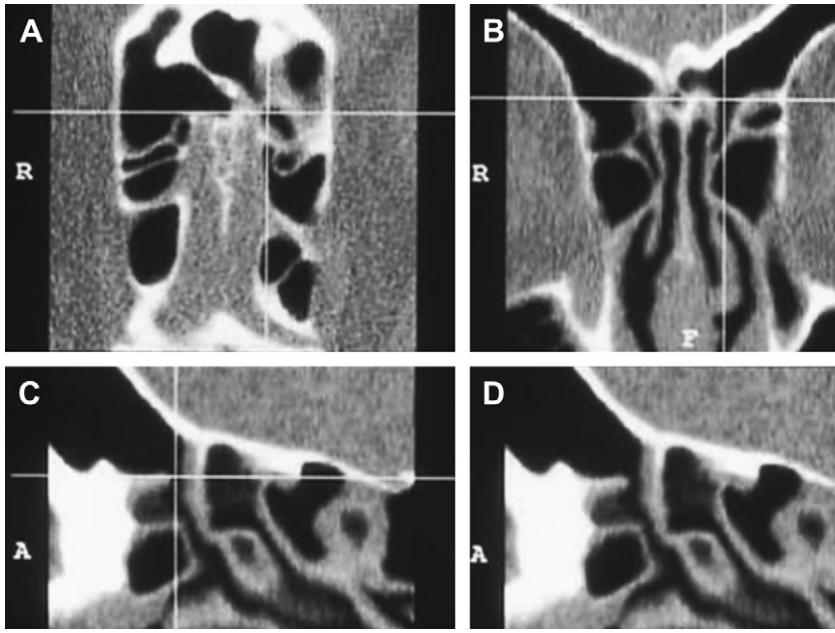

Fig. 1. Multiplanar reconstruction of isotropic imaging data in the axial (*A*), coronal (*B*), and sagittal (*C, D*) planes reveals high-resolution reconstructed imaging information whereby the reconstructed planes are indistinguishable from the acquisition plane. The cross hairs (*A–C*) reveal the ease of cross-referencing anatomic information.

In-office Considerations

The implementation of this technology in a rhinologic office would be more convenient for patients requiring the study, in that it would preclude the need to go through the effort of an additional office appointment. Although the immediate availability of the imaging data improves physician convenience, there are additional factors that need to be considered before adding this equipment to an ear, nose, and throat (ENT) office. The financial considerations regarding the equipment purchase are beyond the scope of this article, which addresses only technical issues.

Before a practice considers acquiring CBCT technology, perhaps the first issue to be considered is whether or not a facility is capable of housing the equipment. As CBCT emits radiation, there are radiation safety considerations, which must be evaluated on a state-by-state basis, as laws vary. Radiation monitoring is important to minimize exposure to the office staff and the general public, requiring proper structural shielding of the equipment to limit the scatter radiation beyond the space housing the equipment.

Most scanners permit the manipulation and viewing of the acquired data at the workstation, but if there is a desire to view images at other locations, a high-speed network must be in place. The amount of data acquired is often large and, depending on the volume of the practice, considerations must be made in regard to data storage. Accessibility of the images from multiple locations, such as office, operating room, and so forth, requires the use of a picture archiving and communications system and compatibility of this equipment with existing equipment should be considered.

It is also important to consider who will actually be acquiring the images. In most cases, a licensed CT technologist is needed to operate the equipment. Furthermore,

Fig. 2. Triplanar display of CBCT data in the coronal (*A*), sagittal (*B*), and axial (*C*) planes demonstrating good resolution of the bony morphology of the nasal cavity and paranasal sinuses.

who will interpret the imaging information? Although dental specialists may be well trained in the interpretation of the dental applications and otolaryngologists in sinus applications, what about nondental and nonsinus lesions that occasionally are present? The lack of soft tissue contrast, hence the inability to diagnose soft tissue lesions in the paranasal sinuses and orbits, is a significant limitation that has the potential to increase the vulnerability of practitioners. Liability issues regarding ''missed'' diagnoses need to be considered and need to be addressed in the implementation process of this diagnostic equipment. Lastly, but of equal importance, is the consideration of the frequency of use of the equipment. Having the equipment on the premises of an office makes it convenient to evaluate patients with chronic sinusitis with this technology. The physician-owner of the equipment needs to address possible queries regarding ''overutilization'' and ''self-referral.'' Strict guidelines regarding this issue should be established at the time of implementation of this technology to show a planned approach to the CT usage and therefore avoid possible criticisms that may be raised.

Radiation Considerations

To measure radiation emitted by MDCT scanners in a standardized fashion, CT dose-index (CTDI) and dose-length product have been developed. Approximate radiation equivalent doses related to diagnostic procedures are provided in **Table 1**.[2] The same general radiation principles are considered when comparing CBCT to MDCT but conventional metrics, such as CTDI and dose-length product, cannot be directly

Table 1
Radiation dose comparison

Diagnostic Procedure	Effective Dose (mSv)	Number of Equivalent Posteroanterior Chest Radiographs for Equivalent Dose	Time Period for Equivalent Effective Dose from Natural Background Radiation
Posterioanterior chest radiograph	0.02	1	2.4 days
Skull radiograph	0.07	4	8.5 days
Lumbar spine	1.30	65	158 days
Intravenous pyelogram	2.50	125	304 days
Upper gastrointestinal series	3.00	150	1.0 year
Barium enema	7.00	350	2.3 years
CT head/sinuses	2.00/0.96	100/48	243/100 + days
CT abdomen	10.00	500	3.3 years

Data from FDA. Available at: www.fda.gov/cdrh/ct/risks.html.

applied to CBCT because of altered beam geometry and differences in x-ray scatter profiles. In addition, the standard phantoms used do not capture the expanded Z-axis beam generated by CBCT that potentially results in significant underestimation of the dose associated with CBCT. An additional complicating factor is that the highest radiation dose in CBCT is at the center of the field, with diminished radiation toward the periphery. For these reasons, volumetric CTDI and dose-length product have been introduced to estimate radiation exposure with CBCT but as yet there is no universally applicable and standardized measure available. Nonetheless, actual dose measurements are obtained with volumetric indices using 18-cm phantoms with a few additional centimeters to incorporate scatter radiation that inevitably are encountered. Comparisons between CBCT and traditional MDCT have been performed (**Table 2**). To maintain the same signal to noise at thinner slice sections, more radiation dose must be used. Published reports indicate that the effective dose varies for various full field-of-view (FOV) CBCT devices, ranging from 0.29 to 0.477 mSv, depending on the type and model of CBCT equipment, the duration of exposure, and FOV selected (see **Table 2**). Comparing these doses with multiples of a single panoramic dose or background equivalent radiation dose, CBCT provides an equivalent patient radiation dose of 5 to 74 times that of a single film–based panoramic x ray or 3 to 48 days of background radiation. The use of additional personal protection (thyroid collar) can substantially reduce the dose by up to 40%.

Table 2
Cone beam CT effective doses for paranasal sinus procedures

Current (mA)	Duration of Exposure (Seconds)	Effective Dose (mSv)
1	7.8	0.03
3.8	7.8	0.10
3.8	20	0.20
3.8	40	0.55

Comparison with patient dose reported for maxillofacial/sinus imaging by MDCT, approximately 1.0 mSv, indicates that CBCT provides a dose reduction. It is not yet clear, however, whether or not the reported degree of dose reduction will be realized in routine clinical settings.

APPLICATIONS OF CONE BEAM CT

Given the ease with which it evaluates the maxillofacial area and its bony resolution, CBCT is used in the assessment of bony and dental pathologic conditions, including fracture, structural maxillofacial deformity, preoperative assessment of impacted teeth, and the temporomandibular joints.[3] It is also used to evaluate availability of bone for implant placement. The technology can also be used to assist in the computer-aided design and manufacture of implant prosthetics,[4] although less than perfect results have been reported with model-forming capability.[5]

It is only natural to expect that CBCT-generated images can be used for surgical navigation during endoscopic sinus surgery. The accuracy of the existing intraoperative stereotactic guidance systems using CBCT images has not been thoroughly investigated; however, some preliminary work suggests feasibility in this regard.[6] The limited FOV and inability to include all fiducial markers seem to be the main practical barrier in front of CBCT's use for all sinus procedures. Regarding endoscopic sinus and skull base surgery, there has been an increasing need for efficient intraoperative real-time imaging, which would show the anatomic changes resulting from surgery. A C-arm–mounted CBCT affords a means to address this need. It provides excellent morphologic localization with high spatial orientation of vital structures during surgery with a potential to increase surgical precision and decrease surgical complications and the need for a repeated surgical procedure, which would otherwise be unforeseen without the use of this instrumentation.[7–10]

MRI TECHNIQUE

The most significant advantage of MRI over CT is its superior contrast resolution, which allows differentiation of sinus inflammatory disease from mass lesions, brain, and orbital structures. Evaluation of neoplastic and invasive inflammatory processes of the paranasal sinuses is best accomplished by MRI. MRI, however, often fails to evaluate the integrity of the bony architecture precluding its use as a roadmap to guide FESS.

T1- and T2-weighted MRI obtained in axial and coronal planes provide a satisfactory evaluation of the sinuses and their mucosa. Contrast-enhanced (gadolinium-diethylenetriamine pentaacetic acid), fat-saturated, T1-weighted images are indispensable for a more comprehensive examination, especially in patients with noninflammatory sinus pathology.

ANATOMY

An understanding of the physiology of the nasal cycle and the mucocilliary clearance of the respective paranasal sinuses is a requisite for understanding the osteomeatal chanels, which provide an intercommunication between the nasal cavity and the paranasal sinuses. The anatomic evaluation needs to focus on the three tight spots: the frontal recess, the infundibulum–middle meatus, and the sphenoethmoid recess.

The frontal sinus drainage pathway is the most complex. The bottom portion of the hourglass-shaped frontal sinus drainage pathway is the frontal recess and also one of the narrowest channels of this outflow tract (the first tight spot) (**Fig. 3**). The structures

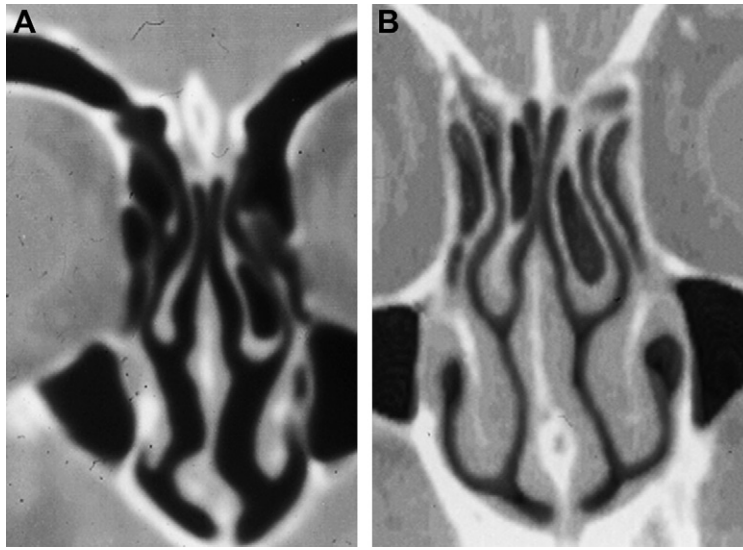

Fig. 3. Coronal CT image in the plane of the frontal recess (*A*) and the corresponding 3-D image (*B*), demonstrating the most anterior tight spot.

adjacent to the frontal recess are the agger nasi cell anteriorly, the ethmoid bulla posteriorly, and the uncinate process inferiorly. The agger nasi cell is an ethmoturbinal remnant, which is present in almost all patients. It is aerated and represents the most anterior ethmoid air cell. It, and frontal cells, usually border the frontal recess; thus, its size may directly influence the patency of the frontal recess and the anterior middle meatus. Anteriorly, the uncinate process fuses with the posteromedial wall of the agger nasi cell and the posteromedial wall of the nasolacrimal duct. Laterally, the free edge of the uncinate process delimits the infundibulum, which is the air passage that connects the maxillary sinus ostium to the middle meatus (the second tight spot).

The superior attachment of the uncinate process has three major variations that determine the anatomic configuration of the frontal recess and its drainage.[11] These variations are

- The uncinate process may extend laterally to attach to the lamina papyracea or the ethmoid bulla, forming a terminal recess of the infundibulum; the frontal recess opens directly to the middle meatus (recessus terminalis).
- The uncinate process may extend medially and attach to the lateral surface of the middle turbinate.
- The uncinate process may extend medially and superiorly to attach directly to the skull base.

In the latter two forms, the frontal recess drains to the infundibulum (recessus frontalis).

The sphenoethmoidal recess (the third tight spot) receives drainage from the posterior ethmoid cells and the sphenoid sinus. It lies just lateral to the nasal septum and leads to the posterior aspect of the superior meatus. The sphenoethmoidal recess is visualized on coronal images but is best evaluated in the sagittal and axial planes.

Using a coronal CT scan, the anatomy of the frontal recess, infundibulum, and middle meatus can be visualized. This is crucial for proper diagnosis and treatment.

Using the real-time multiplanar reconstruction capabilities of modern imaging workstations, understanding of the complex anatomy of these regions can be advanced considerably. The authors found oblique coronal reconstructions with 20° craniocaudal angulation and oblique sagittal reconstructions with 5° to 10° lateromedial angulation particularly helpful in demonstrating the frontal-recess–agger nasi cell–uncinate process relationship. Routine axial images show the sphenoethmoidal recess to the authors' satisfaction but minimally obliqued sagittal reconstructions best demonstrate the sphenoethmoidal recess–superior meatus relationship.

The authors prefer to evaluate the imaging information starting with the most anterior images showing the frontal sinuses and systematically proceeding posteriorly through the sphenoid sinus specifically studying the anatomy surrounding the tight spots. With completion of this task, an evaluation focusing on the nasal septum and proceeding laterally affords additional information regarding the osteomeatal channels, specifically the turbinate relationship to the uncinate process, frontal cells, and anterior and posterior ethmoid cells.[12,13]

APPEARANCE OF RHINOSINUSITIS

The most common indication for sinus imaging is chronic rhinosinusitis (CRS). CT is the imaging standard for evaluation of CRS.[14] The CT signs suggestive of CRS include diffuse or focal mucosal thickening, with partial or complete opacification of the paranasal sinuses; bone remodeling with uniform thickening caused by osteitis from adjacent chronic mucosal inflammation; and polyposis. Thickening and sclerosis of the bony walls of the sinuses are at least in part secondary to the spread of the inflammation through the haversian system within the bone.[15,16]

The distribution of the inflammatory mucosal changes in the nasal cavity and sinuses may provide a clue to the focus of mechanical obstruction, which can be pinpointed by evaluating the sinus drainage pathways. Although CT provides excellent information about the extent and distribution of mucosal disease and the status of the nasal air passages, it does not yield much information regarding the cause of the changes (eg, infection, allergies, granulomatous inflammation, postsurgical scarring, and so forth).

In the acute state, the viscosity of the inflammatory process is of intermediate attenuation on CT (10–25 HU). In the more chronic state, sinus secretions become thickened and concentrated, and the CT attenuation increases, with density measurements of 30 to 60 HU.[17] In the acute state, the obstruction of a specific sinus is followed by a circumferential mucosal edema/inflammation and fluid exudation, represented on CT by an air fluid level and uniform circumferential soft tissue thickening. Contrasted CT and T1-weighted MRI show a uniform uninterrupted enhancement adjacent to the peripheral sinus bony outline. This is characteristic of an inflammatory process within the paranasal sinuses.

Antrochoanal and sphenochoanal polyps appear as well-defined masses that arise from the maxillary or sphenoid sinus and extend to the choana through the middle meatus or sphenoethmoid recess, respectively. They can present as nasopharyngeal masses. It is important to recognize their origin and relationship to the maxillary or sphenoid ostium in treatment planning.

Retention cysts are common incidental findings on imaging studies and are seen as well-defined rounded masses, typically on the maxillary sinus floor. Their clinical significance is not clear.[18] They may become symptomatic if large enough to interfere with drainage pathways.[19]

Mucocele, a complication of CRS, results from a persistant obstruction of the sinus drainage and subsequent expansion of the sinus. Mucoceles are seen more commonly in the ethmoid and frontal sinuses and present with symptoms secondary to compression of the adjacent structures, in addition to the usual symptoms of CRS.

On MRI the appearance of AFS is due to the concentration of feromagnetic elements as described by Zinreich and colleagues,[20] and demonstrated in **Fig. 4**. Som and Curtin[17] describe four patterns of MRI signal intensity that can be seen with chronic sinusitis:

- Hypointense on T1-weighted images and hyperintense on T2-weighted images with a protein concentration of less than 9%
- Hyperintense on T1-weighted images and hyperintense on T2-weighted images with total protein concentration increased to 20% to 25%
- Hyperintense on T1-weighted images and hypointense on T2-weighted images with total protein concentration of 25% to 30%
- Hypointense on T1-weighted images and T2-weighted images with a protein concentration greater than 30% and inspissated secretions in an almost solid form

MRI of inspissated secretions (ie, those with protein concentrations greater than 30%) may have a pitfall in that the signal voids on T1- and T2-weighted images may look identical to normally aerated sinuses.

The correlation between patient symptoms and CT findings is difficult to determine partly because chronic mucosal inflammation may be present without CT findings and asymptomatic persons can have abnormal CT scans. Several studies failed to show a correlation between symptom severity and severity of CT findings.[21–25] In particular, symptoms, such as headache and facial pain, do not correlate with CT findings at all.[26,27] A positive correlation between the severity of symptoms and CT findings may be demonstrated when certain symptoms and negative CT examinations are eliminated.[28,29] The nasal endoscopy findings correlate with CT findings, although the correlation is less than perfect.[24,30,31] The positive predictive value of abnormal endoscopy for abnormal CT is greater than 90%, whereas the negative predictive value of normal endoscopy for normal CT is only 70%.[24,26]

The impact of CT on treatment decision was evaluated in a small study.[32] CT changed the treatment in one third of the patients and allowed more agreement on treatment plan among ENT surgeons.[32]

NEOPLASMS OF THE SINONASAL CAVITIES

Squamous cell carcinoma arising from the sinonasal epithelium accounts for 80% of the malignant tumors seen in this area. Adenocarcinomas arising from the minor

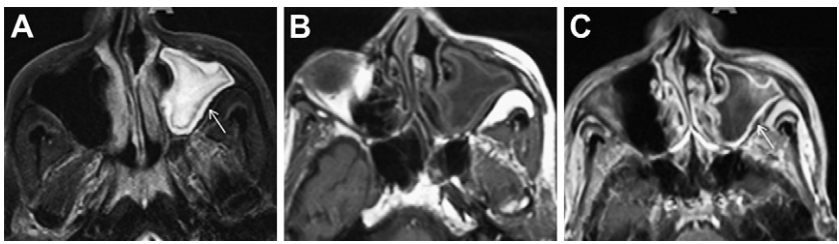

Fig. 4. T2-weighted image (*A*), T1-weighted image (*B*), and postcontrast T1-weighted image. (*C*) These images reveal the typical acute inflammatory change with sinus contents showing fluid-like signal and enhancing mucosa (*arrow*).

salivary glands interspersed in the sinonasal mucosa account for up to 10% of the malignant tumors. Melanomas are responsible for 5% of sinonasal malignant tumors. Less common malignant tumors of the sinonasal cavities include olfactory neuroblastoma, lymphomas, and sarcomas. A detailed discussion of these individual entities is beyond the scope of this article.

On CT, neoplasms are recognized by their invasive character and bone erosion. Focal bone erosion with or without expansion is evident. Depending on size and extension, the mass may erode through the bony confines of a particular sinus and invade the tissues peripheral to the sinus bony architecture. The precise extension can be best determined with a contrast-enhanced MRI study. The mass is usually of lower signal intensity and its contrast enhancement is less than that of an inflammatory process. The uniform enhancement seen peripherally within a sinus cavity with inflammation is interrupted as the mass extends beyond the confines of the sinus cavity. Additionally, certain characteristics are associated with specific neoplasms. Peripheral cysts are associated with esthesioneuroblastomas. A serpiginous cerebral sulcal–like enhancement is associated with inverted papilomas.

SUMMARY

Two and a half decades after the introduction of FESS in the United States, the role of imaging with respect to this surgical procedure is the information it provides regarding the anatomic detail of the nasal cavity and paranasal sinuses. The imaging information affords surgical planning and guidance. Furthermore, when considering the application of CT and MRI, the information derived from these technologies helps narrow the differential diagnosis and helps define the causes of various pathologic entities confronted in this area.

As FESS has evolved since 1985, so has imaging technology and its application with regards to this surgery. Of significant note is the introduction of image-guided surgery. Image guidance further revolutionized the use of imaging information in that it provided a direct confirmation of anatomic structures and improved the guidance and safety of the surgical act.

The introduction of CBCT begins a new phase of change in the use of imaging for the evaluation of maxillofacial pathology. Its presence in the office environment addresses issues related to the patient and physician ''convenience factor.'' The radiation exposure and diagnostic issues are new topics with which ENT offices need to deal (in most instances for the first time), to adhere to the various regulatory measures and potential risks introduced by this technology in the in-office setting.

Regarding the use of CBCT in the OR setting, early results seem to show augmented benefits provided by image-guided surgery, in that it provides confirmation of the extent of surgery before patients leave the operating room, therefore providing accurate confirmation of the surgical objective.

REFERENCES

1. Mozzo P, Procacci C, Tacconi A, et al. A new volumetric CT machine for dental imaging based on the cone-beam technique: preliminary results. Eur Radiol 1998;8:1558–64.
2. FDA. Available at: www.fda.gov/cdrh/ct/risks.html.
3. Thomas SL. Application of cone-beam CT in the office setting. Dent Clin North Am 2008;52:753–9, vi.
4. Scarfe WC, Farman AG. What is cone-beam CT and how does it work? Dent Clin North Am 2008;52:707–30, v.

5. Hassan B, van der Stelt P, Sanderink G. Accuracy of three-dimensional measurements obtained from cone beam computed tomography surface-rendered images for cephalometric analysis: influence of patient scanning position. Eur J Orthod 2009;31:129–34.
6. Eggers G, Muhling J, Hofele C. Clinical use of navigation based on cone-beam computer tomography in maxillofacial surgery. Br J Oral Maxillofac Surg 2009.
7. Chan Y, Siewerdsen JH, Rafferty MA, et al. Cone-beam computed tomography on a mobile C-arm: novel intraoperative imaging technology for guidance of head and neck surgery. J Otolaryngol Head Neck Surg 2008;37:81–90.
8. Bachar G, Barker E, Nithiananthan S, et al. Three-dimensional tomosynthesis and cone-beam computed tomography: an experimental study for fast, low-dose intraoperative imaging technology for guidance of sinus and skull base surgery. Laryngoscope 2009;119:434–41.
9. Rafferty MA, Siewerdsen JH, Chan Y, et al. Intraoperative cone-beam CT for guidance of temporal bone surgery. Otolaryngol Head Neck Surg 2006;134:801–8.
10. Rafferty MA, Siewerdsen JH, Chan Y, et al. Investigation of C-arm cone-beam CT-guided surgery of the frontal recess. Laryngoscope 2005;115:2138–43.
11. Daniels DL, Mafee MF, Smith MM, et al. The frontal sinus drainage pathway and related structures. AJNR Am J Neuroradiol 2003;24:1618–27.
12. Zammit-Maempel I, Chadwick CL, Willis SP. Radiation dose to the lens of eye and thyroid gland in paranasal sinus multislice CT. Br J Radiol 2003;76:418–20.
13. Tack D, Widelec J, De Maertelaer V, et al. Comparison between low-dose and standard-dose multidetector CT in patients with suspected chronic sinusitis. AJR Am J Roentgenol 2003;181:939–44.
14. Benninger MS, Ferguson BJ, Hadley JA, et al. Adult chronic rhinosinusitis: definitions, diagnosis, epidemiology, and pathophysiology. Otolaryngol Head Neck Surg 2003;129:S1–32.
15. Perloff JR, Gannon FH, Bolger WE, et al. Bone involvement in sinusitis: an apparent pathway for the spread of disease. Laryngoscope 2000;110:2095–9.
16. Khalid AN, Hunt J, Perloff JR, et al. The role of bone in chronic rhinosinusitis. Laryngoscope 2002;112:1951–7.
17. Som PM, Curtin HD. Chronic inflammatory sinonasal diseases including fungal infections. The role of imaging. Radiol Clin North Am 1993;31:33–44.
18. Bhattacharyya N. Do maxillary sinus retention cysts reflect obstructive sinus phenomena? Arch Otolaryngol Head Neck Surg 2000;126:1369–71.
19. Hadar T, Shvero J, Nageris BI, et al. Mucus retention cyst of the maxillary sinus: the endoscopic approach. Br J Oral Maxillofac Surg 2000;38:227–9.
20. Zinreich S, Kennedy D, Malat J, et al. Diagnosis with CT and MR imaging. Radiology 1998;169(2):439–44.
21. Bhattacharyya T, Piccirillo J, Wippold FJ 2nd. Relationship between patient-based descriptions of sinusitis and paranasal sinus computed tomographic findings. Arch Otolaryngol Head Neck Surg 1997;123:1189–92.
22. Ashraf N, Bhattacharyya N. Determination of the "incidental" Lund score for the staging of chronic rhinosinusitis. Otolaryngol Head Neck Surg 2001;125:483–6.
23. Stewart MG, Sicard MW, Piccirillo JF, et al. Severity staging in chronic sinusitis: are CT scan findings related to patient symptoms? Am J Rhinol 1999;13:161–7.
24. Stankiewicz JA, Chow JM. Nasal endoscopy and the definition and diagnosis of chronic rhinosinusitis. Otolaryngol Head Neck Surg 2002;126:623–7.
25. Stankiewicz JA, Chow JM. A diagnostic dilemma for chronic rhinosinusitis: definition accuracy and validity. Am J Rhinol 2002;16:199–202.

26. Rosbe KW, Jones KR. Usefulness of patient symptoms and nasal endoscopy in the diagnosis of chronic sinusitis. Am J Rhinol 1998;12:167–71.
27. Mudgil SP, Wise SW, Hopper KD, et al. Correlation between presumed sinusitis-induced pain and paranasal sinus computed tomographic findings. Ann Allergy Asthma Immunol 2002;88:223–6.
28. Arango P, Kountakis SE. Significance of computed tomography pathology in chronic rhinosinusitis. Laryngoscope 2001;111:1779–82.
29. Kenny TJ, Duncavage J, Bracikowski J, et al. Prospective analysis of sinus symptoms and correlation with paranasal computed tomography scan. Otolaryngol Head Neck Surg 2001;125:40–3.
30. Rose GE, Sandy C, Hallberg L, et al. Clinical and radiologic characteristics of the imploding antrum, or "silent sinus," syndrome. Ophthalmology 2003;110:811–8.
31. Kennedy DW, Wright ED, Goldberg AN. Objective and subjective outcomes in surgery for chronic sinusitis. Laryngoscope 2000;110:29–31.
32. Anzai Y, Yueh B. Imaging evaluation of sinusitis: diagnostic performance and impact on health outcome. Neuroimaging Clin N Am 2003;13:251–63, xi.